

QLEDs for displays and solid-state lighting

Geoffrey J. Supran, Yasuhiro Shirasaki, Katherine W. Song, Jean-Michel Caruge, Peter T. Kazlas, Seth Coe-Sullivan, Trisha L. Andrew, Moungi G. Bawendi, and Vladimir Bulović

The mainstream commercialization of colloidal quantum dots (QDs) for light-emitting applications has begun: Sony televisions emitting QD-enhanced colors are now on sale. The bright and uniquely size-tunable colors of solution-processable semiconducting QDs highlight the potential of electroluminescent QD light-emitting devices (QLEDs) for use in energy-efficient, high-color-quality thin-film display and solid-state lighting applications. Indeed, this year's report of record-efficiency electrically driven QLEDs rivaling the most efficient molecular organic LEDs, together with the emergence of full-color QLED displays, foreshadow QD technologies that will transcend the optically excited QD-enhanced products already available. In this article, we discuss the key advantages of using QDs as luminophores in LEDs and outline the 19-year evolution of four types of QLEDs that have seen efficiencies rise from less than 0.01% to 18%. With an emphasis on the latest advances, we identify the key scientific and technological challenges facing the commercialization of QLEDs. A quantitative analysis, based on published small-scale synthetic procedures, allows us to estimate the material costs of QDs typical in light-emitting applications when produced in large quantities and to assess their commercial viability.

Colloidal quantum-dots: High-quality visible and infrared light sources

Colloidal quantum dots (QDs) are solution-processed nanoscale crystals of semiconducting materials. They emit bright, pure, and tunable colors of light, making them excellent candidates for color centers in next-generation display and solid-state lighting (SSL) technologies.[1] As illustrated in **Figure 1**a and described in the other articles in this issue, their narrow emission spectra can be readily tuned throughout the visible and near-infrared (NIR) spectrum via both quantum size effects and changes in chemical composition.[2–4]

For visible applications, CdSe-based QDs are currently the material of choice;[3,5–7] their saturated emission spans the visible spectrum, delineating a large potential color gamut that approaches that of the human eye[8] (Figure 1b). For this reason, QDs have already begun to find commercial applications as optically excited color enhancers: Sony's 2013 line of Triluminos liquid crystal display (LCD) televisions (Figure 1b, inset) use edge-mounted red and green QDs from QD Vision to optically down-convert some of the television's blue LED backlight (absorbing some of the blue light and re-emitting it as red and green light)—optimizing its color balance so that it fulfills >100% of the National Television System Committee (NTSC) television color gamut standard (the color space for broadcast video defined by the NTSC in 1953), compared with ~70% for conventional LCD screens (Figure 1b).[9,10] The result is a television picture with color quality comparable to that of organic LED (OLED) screens, but achieved at the cost of an LCD display. 3M and Nanosys are together exploring similar strategies using their Quantum Dot Enhancement Film.[11] Analogous approaches have also been utilized in backlights in high-color-quality white LED SSL, such as QD Vision's Quantum Light developed in collaboration with Nexxus Lighting.[1,8]

Geoffrey J. Supran, Massachusetts Institute of Technology; gjsupran@mit.edu
Yasuhiro Shirasaki, Massachusetts Institute of Technology; yshir@mit.edu
Katherine W. Song, Massachusetts Institute of Technology; kwsong@mit.edu
Jean-Michel Caruge, QD Vision; jcaruge@qdvision.com
Peter T. Kazlas, QD Vision; pkazlas@qdvision.com
Seth Coe-Sullivan, QD Vision; scoe-sullivan@qdvision.com
Trisha L. Andrew, University of Wisconsin–Madison; tandrew@chem.wisc.edu
Moungi G. Bawendi, Massachusetts Institute of Technology; mgb@mit.edu
Vladimir Bulović, Massachusetts Institute of Technology; bulovic@mit.edu
DOI: 10.1557/mrs.2013.181

© 2013 Materials Research Society

https://doi.org/10.1557/mrs.2013.181 Published online by Cambridge University Press

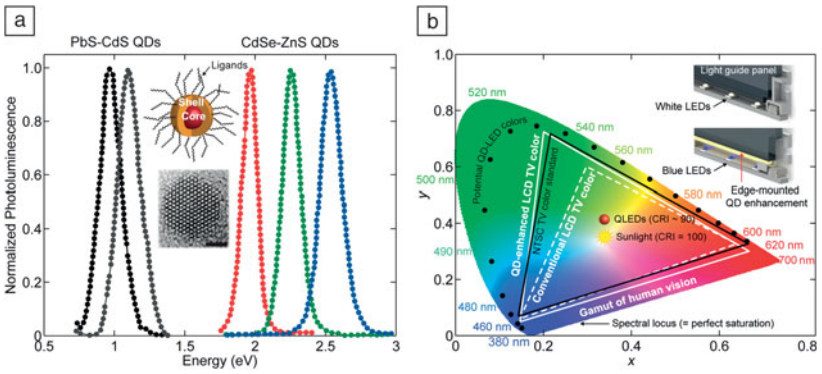


Figure 1. Pure and tunable colloidal quantum dot (QD) light emission for display applications. (a) Normalized photoluminescence (PL) spectra of visible-emitting CdSe-ZnS core–shell QDs and near infrared-emitting PbS-CdS core–shell QDs, demonstrating size- and composition-tunable emission colors. Quantum dot light-emitting device (QLED) electroluminescence typically closely matches the corresponding PL spectra. Upper inset: Schematic of a core–shell colloidal QD passivated by organic ligands. Lower inset: High-resolution transmission electron microscope image of a CdSe QD (scale bar, 1.5 nm). (b) The CIE chromaticity diagram, created by the International Commission on Illumination (CIE) in 1931, allows color quality to be quantified by mapping colors visible to the human eye in terms of hue and saturation. The color gamut of conventional LCD televisions (upper inset and dashed white line) is enhanced by ~50% by edge-mounted QDs (lower inset and solid white line) so as to match 100% of the NTSC television color gamut standard (black line). An ideal combination of red-green-blue QLED sources has the potential to generate the colors defined by the black dots in the figure, or to serve as a high color-quality (CRI ~90) white light source. (a) Background, Reference 8; lower inset, Reference 87.

Among the candidate large-area planar light-emitting materials, QDs and organic dyes stand out, as they enable room temperature processing and non-epitaxial deposition. Indeed, as visible-light emitters, OLEDs are already a relatively mature technology with a sizeable market share. Yet the extendibility of QD emission into the NIR—currently spearheaded by lead chalcogenide-based QDs[12–14]—is a significant technological advantage over organic dyes. Whereas organic molecules have negligible optical activity beyond wavelengths of $\lambda = 1$ μm (their photoluminescence (PL) quantum yield, η_{PL}, a measure of their intrinsic brightness, is <5% at these wavelengths) and exhibit poor chemical and photo-stability, QDs are relatively stable[1] and retain η_{PL} >70% in the visible[15] (>95% for red QDs[16]) and >50% throughout the NIR.[15,17–20]

QDs also match the solution processability of organic dyes—opening up the possibility for large-area and flexible displays and form-factors tailored for incorporation into SSL applications (e.g., see the inset of Figure 1b)—and generally surpass them in terms of stability.[1] Their promise is evidenced by the large number of start-up companies and major corporations, such as QD Vision, Nanosys, Sony, 3M, LG Innotek, Samsung, Philips Lumileds Lighting Company, and Avago, developing colloidal QD-enhanced displays and SSL sources.[21] But while the existing applications under commercial exploration harness the optically excited emission (PL) of QDs, one can envisage the development of large-area QLED flat-panel displays reliant on the electrically induced emission (electroluminescence, EL) of colloidal QDs, which is a target also being pursued commercially. With the global flat-panel display market exceeding USD$80 billion in 2011,[22] and with lighting constituting 20% of US electricity consumption,[21] the economic and environmental incentives are clear.

Evolution of electrically driven QLEDs

A typical electrically driven QD light-emitting device (QLED) comprises two electrodes, which inject charge into a series of active layers sandwiched between them (e.g., see **Figure 2**a). Since their initial demonstration in 1994,[23] the performance of QLEDs has improved dramatically. This has, in part, been the result of evolving device architectures, which we have previously classified into the four "types" depicted in the inset of **Figure 3**a.[1] Figure 3a maps the progression in QLED performance in terms of external quantum efficiency (EQE), which is defined as the ratio of the number of photons emitted by the LED in the viewing direction to the number of electrons injected. (The EQEs in Figure 3a are for orange/red-emitting devices, which are the most prevalent class of visible-emitting QDLEDs reported to date. We note that Lee et al. recently demonstrated blue-emitting QDLEDs with record EQEs as high as 7.1%[105]). EQE is directly proportional to power conversion efficiency and is therefore a key metric for SSL and displays.

Type I: QLEDs with polymer charge transport layers

The earliest generation of QLEDs (Type I) were a natural progression from polymer LEDs, comprising active layers of either bilayers or blends of CdSe QDs and polymers.[23,24] Their EQEs were low (typically <0.1%) mainly because QDs were forced to play dual roles of charge conduction and light emission; while thick wide-bandgap shells and long organic ligands generally serve to passivate a QD and enhance its η_{PL}, they also markedly detract from the mobility of the QD film.

Type II: QLEDs with organic small molecule charge transport layers

Type II QLEDs were first introduced by Coe et al. in 2002 and comprise a monolayer of QDs at the interface of a bilayer OLED.[25] These devices demonstrated record EQEs of 0.5%, an efficiency that has since been augmented by an additional factor-of-ten through optimizations. The enhanced performance was attributed to the use of a single monolayer of QDs (enabled by the development of spin-coating[25] and microcontact printing[26–28] techniques), which decouples the luminescence process in the QDs from charge transport through the organic layers.[25,27,29–32]

https://doi.org/10.1557/mrs.2013.181 Published online by Cambridge University Press

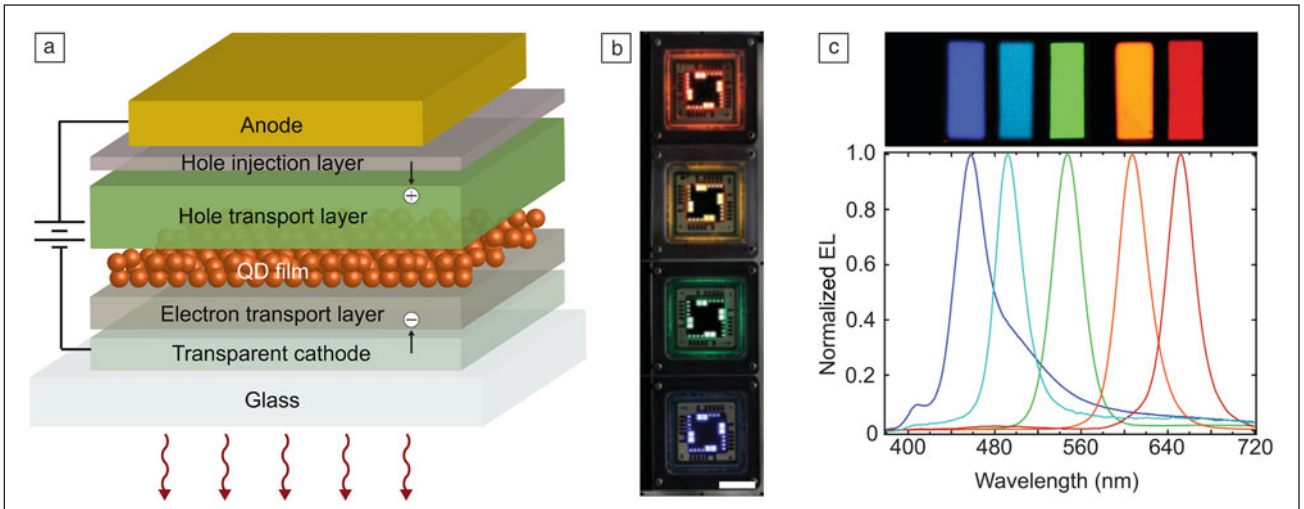


Figure 2. Prototypical quantum dot light-emitting device (QLED) design and operation. (a) Inverted hybrid organic-QD-inorganic Type IV QLED structure that has risen to prominence owing to its record efficiencies and brightness. It typically comprises a few monolayers of QDs sandwiched between an inorganic metal oxide electron transport layer and an organic hole transport layer. Photographs of tunable electroluminescence (EL) colors from (b) Type IV (scale bar, 2 cm) and (c) Type II QLEDs (together with respective EL spectra).[3]

Type III: QLEDs with inorganic charge transport layers

Type II devices boast all of the advantages of OLEDs, with the added benefits of enhanced spectral purity and tunability, as illustrated by the tunable EL shown in Figure 2b–c. However, Type III QLEDs, which replace the organic charge transport layers (CTLs) of Type II QLEDs with inorganic CTLs, can potentially lead to greater device stability in air[33,34] and should enable the passage of higher current densities and therefore brighter emission. Initial demonstrations of Type III QLEDs based on sputtered metal oxides have indeed displayed high current densities (up to 4 A cm^{-2}), but EQEs to date remain less than 0.1%.[35] Over the past few years, similarly structured all-inorganic (except for organic ligands) QLEDs that operate by the altogether different excitation mechanism of QD ionization have also emerged[1,36,37] (**Figure 4**d).

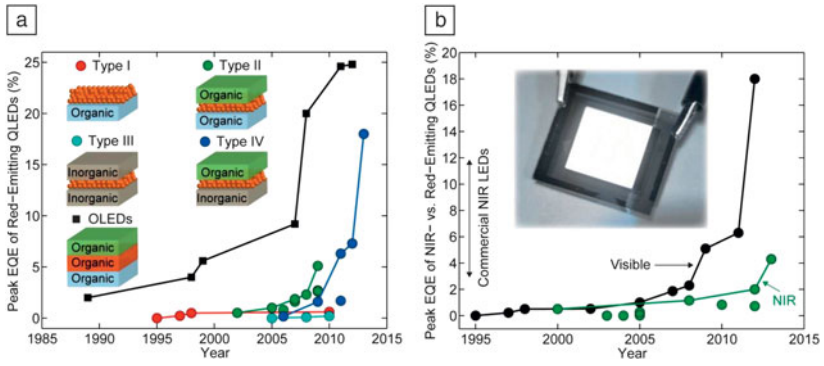


Figure 3. Progression in efficiencies over time of electrically driven visible- and near-infrared (NIR)-emitting quantum dot light-emitting devices (QLEDs). (a) Peak external quantum efficiencies (EQEs) of orange-red-emitting QLEDs (a substantial but non-exhaustive selection from the literature), classified into one of four types, as described in the text and represented schematically in the inset: Type I (References 62, 88–90); Type II (References 3, 4, 25, 32, 44, 63, 66, 67, 91); Type III (References 29, 35, 36); and Type IV (References 5, 7, 39, 43, 78, 92). These are compared with selected orange-red-emitting (phosphorescent) organic LEDs (References 93–96). Solid lines connect new record values. (b) EQEs of NIR ($\lambda > 1$ μm) QLEDs (green) (References 12, 13, 53, 54, 56, 60, 97–100) are compared with the EQE range of commercial NIR LEDs and with record-efficient visible-emitting QLEDs (of all types) from (a) (black). Inset: NIR electroluminescence at a wavelength of $\lambda = 1.1$ μm from a 4 cm^2 NIR QLED viewed through an infrared camera.

Type IV: QLEDs with hybrid organic-inorganic charge transport layers

The hybrid structure of Type IV QLEDs offers a compromise between Type II and Type III QLEDs, often comprising an inorganic metal oxide electron transport layer (notably solution processed ZnO[5,7]) and an organic small molecule hole transport layer.[5,7,38–40] A typical device structure and its corresponding EL are shown in Figure 2a–b. Significant efficiency gains have resulted, with recent visible-emitting QLEDs reaching EQEs as high as 18%[40] (**Figure** 3a and **5**a), approaching those of commercially mature phosphorescent OLEDs[41] as well as the outcoupling-limited EQE ceiling of ~20–25% (without targeted device engineering, the fraction of emitted photons that are coupled out of a planar QD-LED is limited by wave guided and surface plasmon modes to ~5–50%[1]).[42] The brightness of Type IV QLEDs has also reached record levels of 218,800 cd m^{-2}.[7] High-resolution microcontact printing of QD films (>1000 pixels per inch)[26] (Figure 5b) has already enabled

https://doi.org/10.1557/mrs.2013.181 Published online by Cambridge University Press

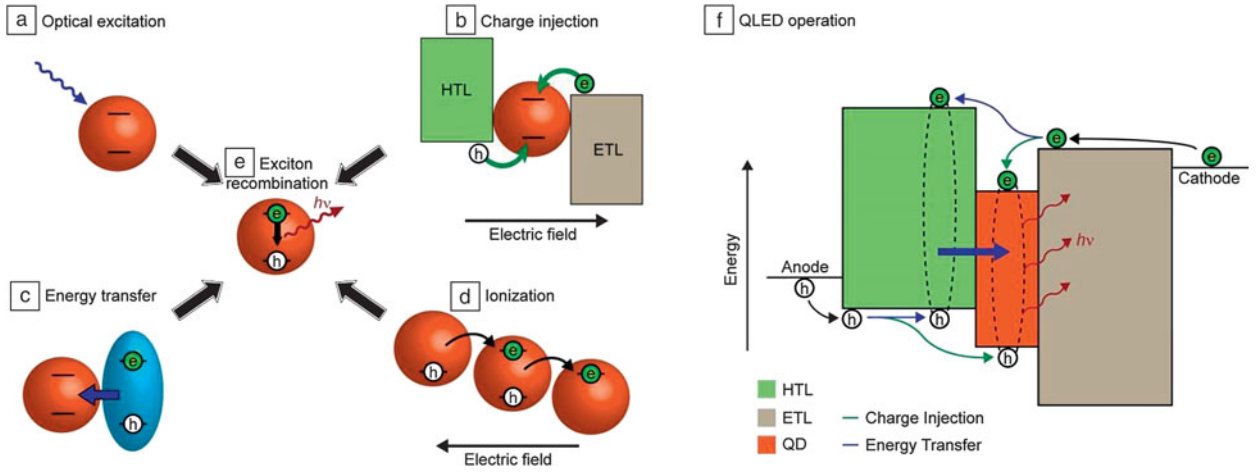


Figure 4. Quantum dot (QD) excitation mechanisms. There are four routes to generating excitons in QDs that have been used in quantum dot light-emitting devices (QLEDs). (a) Optical excitation: An exciton is formed in a QD by absorbing a high-energy photon. (b) Charge injection: Neighboring charge transport layers inject charge carriers directly into a QD. (c) Energy transfer: An exciton is transferred from a nearby donor molecule to a QD via Förster resonant energy transfer. (d) Ionization: A large electric field ionizes an electron from one QD to another, thereby generating a hole. When these ionization events occur throughout a QD film, generated electrons and holes can meet on the same QD to form excitons. (e) Exciton formation is followed by exciton recombination, generating light. (f) Energy band diagram of a typical QLED outlines the two suspected routes to electrical exciton formation in QDs: (green arrows) charge injection; and (blue arrows) energy transfer.

the fabrication of full-color 4-inch QLED displays[43] and, by mixing different compositions[44] or sizes[45] of QDs, white-emitting QLEDs that are highly amenable to SSL have been demonstrated with excellent color quality (color rendering index, CRI ~90 [out of 100]—see Figure 1b). White-emitting QLEDs on flexible substrates (Figure 5c) have also been realized at QD Vision.[1,46]

Beyond Cd-based QDs: Near infrared and non-toxic QLEDs

The paucity of high-η_{PL} NIR molecular and polymeric dyes provides a compelling impetus to extend the EL of QLEDs from the visible into the NIR range (780–2,500 nm): EQEs of OLEDs and polymer LEDs emitting at $\lambda > 1$ μm remain less than 0.3%.[47] NIR-emitting QLEDs boast unique potential: One can envision NIR light sources that can be deposited on any substrate and at lower cost than existing (usually epitaxially grown) IR-emitters finding application in optical telecommunications and computing[19,48] (solution-processability may enable Si-compatibility); bio-medical imaging[19,49,50] (utilizing biological transparency windows between 800 nm and 1700 nm[49]); on-chip bio(sensing) and spectroscopy;[19,51,52] and night-time surveillance and other security applications (Figure 5d). Most NIR QLEDs have been based on Type I architectures and core-only NIR (lead chalcogenide) QDs,[12,53–57] with EQEs of up to ~2% reported[12] (Figure 3b). In our laboratory at MIT, we have recently realized devices with efficiencies exceeding 4%[14,58]—more than double the previous record—by transitioning to a Type IV device structure and exploiting the enhanced passivation of core–shell NIR QDs. At QD Vision, NIR QLEDs with active areas of up to 4 cm^2 (Figure 3b, inset) and radiances of up to 18.3 W sr^{-1} m^{-2} have been achieved, comparable to commercial IR LEDs and sufficient to serve as large-area IR illuminators (Figure 5d).

Recently, Cheng et al. described the first Si QD-based LEDs, with very high EQEs of 0.6% (Type I)[59] and 8.6% (Type II),[60] though with a rather blue NIR EL of ~850 nm. Although emission at wavelengths beyond 1 μm may be difficult to achieve with Si QDs (efficient blue and green emitters have also not yet been demonstrated), this new breed of heavy-metal-free QLEDs nevertheless addresses growing concerns regarding the risks* that cations such as cadmium, lead, and mercury pose to our health and to the environment.[1]

Challenges and outlook for QLEDs

Even as QDs begin to penetrate mainstream markets as optical down-converters, there remain key challenges facing electrically driven QLEDs.

QLED operating mechanisms

First, most routes to higher efficiency QLEDs—especially those addressing the quenching and lifetime of QDs under operational conditions—will be predicated on a better understanding of their operating mechanisms. In all four types of

* How much cadmium (Cd) is in a QLED? We can estimate this by assuming (as we will again in the "QLED cost" section later) that a typical QLED might comprise a 5 cm × 5 cm film, 25 nm thick, of hexagonally close-packed CdSe-CdS core–shell QDs separated by ~0.5 nm due to their surrounding organic ligands. Then, the effective density of CdSe-CdS QDs with a diameter of 4 nm and a shell thickness of 2 nm is 3.5 g cm^{-3}, which translates to a mass of 0.16 mg of CdSe-ZnS and therefore 63 μg of Cd. This is comparable to one's daily Cd intake: the age-weighted mean Cd intake for males in the United States is 0.35 μg kg^{-1} day^{-1}, or 24.5 μg day^{-1} for a 70 kg male.[104]

https://doi.org/10.1557/mrs.2013.181 Published online by Cambridge University Press

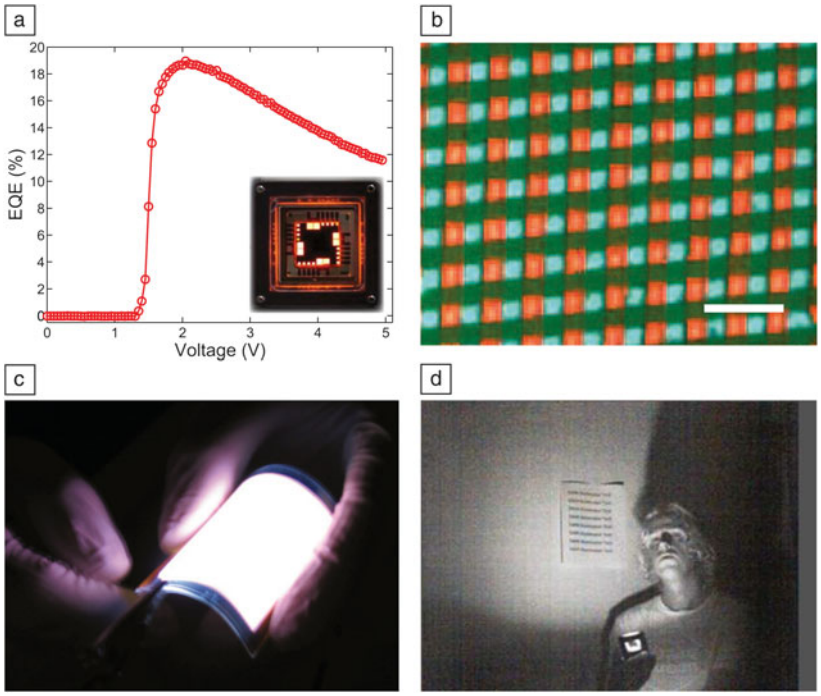


Figure 5. State-of-the-art quantum dot light-emitting devices (QLEDs). (a) External quantum efficiency (EQE) versus applied voltage for record high performance (peak EQE of 18%) red-emitting (photograph in inset) QLEDs. (b) The first demonstration of red-green-blue electroluminescence from (Type II) QLED pixels, patterned using microcontact printing (scale bar, 100 μm). (c) Flexible white-emitting Type II QLED. (d) Large-area infrared illumination by an infrared-emitting QLED, as seen through an infrared camera. (a) Adapted with permission from Reference 40. (b) Adapted with permission from Reference 26. (c) Adapted with permission from Reference 46.

QLEDs, QD EL has been speculated to be driven by direct charge injection[29] (Figure 4b), Förster resonant energy transfer (FRET) (Figure 4c), or both, with the relative contribution of these mechanisms remaining unclear.[5,57,61,62] In the case of direct charge injection, an electron and a hole are injected from CTLs into a QD, forming an exciton that subsequently recombines via emission of a photon (Figure 4f, green arrows). In the FRET scheme, an exciton is first formed on a luminescent CTL. Thereafter, the exciton energy is non-radiatively transferred to a QD via dipole-dipole coupling (Figure 4f, blue arrows).

Studies in our group have indicated that, at least in certain Type II QLED geometries, FRET is the dominant QD excitation mechanism.[32] Yet, for example, the achievement of EQEs >2% in QD monolayer-based devices comprising organic donor materials with very low η_{PL}[63] challenges the universality of the FRET model. Moreover, since Type III and Type IV QLEDs, in contrast with Type II QLEDs, employ QD films thicker than one monolayer (up to ~50 nm), the working mechanism of Type IV QLEDs is more compatible with a charge injection model.

QD PL quenching

From a device efficiency perspective, a second central consideration is QD PL quenching, since EQE is directly proportional to η_{PL}. While our previous review focused on the challenges and opportunities in improving the intrinsic (zero bias) η_{PL} of QDs in QLEDs,[1] there are also ongoing efforts to understand the impact of bias-dependence of QD η_{PL} on EQE.[64,65] This is of interest because application of voltage to QLEDs can lead to further reductions in η_{PL} due to injected-charge-induced Auger recombination[8,36,66,67] and electric field-induced exciton quenching.[63,68–71] A major consequence of these bias-induced instabilities may be a reduction in the operational lifetimes of QLEDs.

By simultaneously measuring the PL and EL of operating QLEDs, our recent work indicates that the roll-off in efficiency typically observed at high applied biases (e.g., see Figure 5a) in a Type IV QLED can be wholly explained by a simultaneous roll-off in QD η_{PL}.[64] From the electric field dependence of QD PL we are able to quantitatively predict the EQE roll-off (**Figure 6**) and therefore to deduce that it is largely governed by electric field-induced QD luminescence quenching, and not carrier leakage or QD charging. Bozyigit et al. have likewise observed a substantial roll-off in QD η_{PL} when the QDs are exposed to an electric field.[65] Transient PL measurements of QDs under varying electric fields[64,65] suggest that the cause of quenching is either a decrease in radiative exciton recombination rate (for example, due to a decrease in the overlap of electron and hole wave functions)[65] or a decrease in the efficiency of thermalized-exciton formation (e.g., trapping of hot charge carriers by QD surface traps).[72,73]

These findings pose a tall order for the redesign of QLEDs with reduced EQE roll-off; efficient QD excitation by FRET[32,74–76] (rather than direct charge injection) may help to decouple the efficiency of exciton formation from η_{PL} so that bias-induced PL quenching can be minimized.

QLED lifetime

Operational lifetime improvements are perhaps the greatest technological hurdle to the commercialization of electrically driven QLEDs. Demonstrations of intrinsic QD PL lifetimes of >14,000 hours and PL thermal stabilities (12% fall-off at 140°C) comparable with red inorganic phosphors[77] already render QDs commercially viable in lower flux/temperature optical down-conversion applications.[10] Yet the lifetimes of today's electrically driven QLEDs (mainly Type IV) operated at initial video brightness (of 100 cd m^{-2}) are usually on the order of only 100 to 1000 hours[5–7,43,78] (>10,000 hours is required for displays) compared with 10^3 to 10^6 hours[79] for state-of-the-art OLEDs. Encouragingly, QD Vision recently reported a Type IV visible-emitting QLED with a half-life

https://doi.org/10.1557/mrs.2013.181 Published online by Cambridge University Press

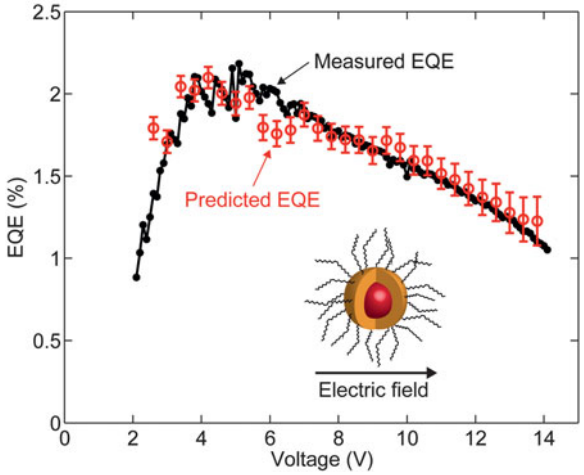


Figure 6. Efficiency roll-off in quantum dot light-emitting devices (QLEDs). Measured (black) and predicted (red) external quantum efficiency (EQE) as a function of voltage for a red-emitting QLED. The roll-off in EQE at high biases commonly observed in QLEDs is shown to be consistent with that predicted by accounting for reductions in QD photoluminescence quantum yield under the associated electric fields in an operating device. Adapted with permission from Reference 64.

(the time after which brightness has fallen to half its initial [time zero] value) of >10,000 hours when operated at 100 cd m^{-2} initial brightness,[77] and have achieved record lifetimes for NIR QLEDs of up to ~1700 hours (at an initial radiance of ~3W sr^{-1} m^{-2}). We have previously outlined some possible strategies for addressing the short lifetimes of most QLEDs,[1] but the absence of in-depth studies focused on QLED stability is conspicuous.

QLED cost

From a manufacturing standpoint, QLEDs may be approximated as QD-enhanced OLEDs. The manufacturing cost of QLEDs can be broadly divided into the cost of raw materials and the fabrication costs of processing these materials. The similarity of the constituent materials of QLEDs and OLEDs means that they are fabricated using a similar toolbox of thin-film processing techniques, so that QLED commercialization would benefit from the manufacturing infrastructure and expertise developed for OLED production. Aside from the QDs themselves, the materials typically employed in QLEDs (metals, metal oxides, and organic small molecules) are also very similar to those found in OLEDs. Their materials costs should therefore be commensurate with those that are enabling the growth of OLED markets and would benefit from their economies of scale.

To estimate the materials costs of QDs typical in light-emitting applications when produced in large quantities, we perform a quantitative analysis based on published small-scale synthetic procedures, which we have previously used to asses the commercial viability of organic materials for photovoltaics.[80] We consider a few of the most common and promising QLED materials and synthetic preparations: red-emitting "legacy" CdSe QDs,[81] "modern" CdSe QDs,[16] "legacy" CdSe-ZnS core–shell QDs,[82] and "modern" CdSe-CdS core–shell QDs[16] (all with trioctylphosphine oxide (TOPO) ligands); NIR-emitting PbS-CdS core–shell QDs (with oleic acid ligands); and PbS QDs (with oleic acid ligands), which are not only commonly used in NIR QLEDs but have also garnered tremendous interest as an active material in QD-based solar cells. The "legacy" and "modern" labels refer to the synthetic recipe evaluated, as discussed later. As detailed in Reference 80, our cost analysis takes into account all of the material inputs to these procedures in order to estimate the total material costs for each type of QD (based on our assembled database of quotations from major chemical suppliers for each of the input materials). As an example, our model for the synthesis of PbS-CdS is represented graphically as a flowchart in **Figure 7**. The first box in the flowchart represents the starting material, lead (II) oxide. Red arrows indicate reagents, green arrows indicate solvents, and blue arrows indicate additional materials required for workup and purification ("crash out"). The indicated quantities of input materials and waste are calculated to produce one kilogram of product.

The materials costs results from our models for each synthetic procedure are summarized in **Table I**. We note that the material costs that we consider represent only one component of the overall cost to produce these materials. In the case of pharmaceutical drugs, for example, materials only account for 20–45% of the cost of drug synthesis. The balance includes contributions for labor, capital, utilities, maintenance, waste treatment, taxes, insurance, and various overhead charges.[80]

We find that the materials costs of visible-emitting "legacy" CdSe QDs ($569–660 g^{-1}; lower value is without workup, upper value is with workup) exceed those of "modern" CdSe QDs ($58–59 g^{-1}) by an order-of-magnitude as a consequence of similarly sizeable differences in the costs of reagents, solvents, and workup materials. This reflects the 20-year evolution in synthesis procedures that has led to the use of

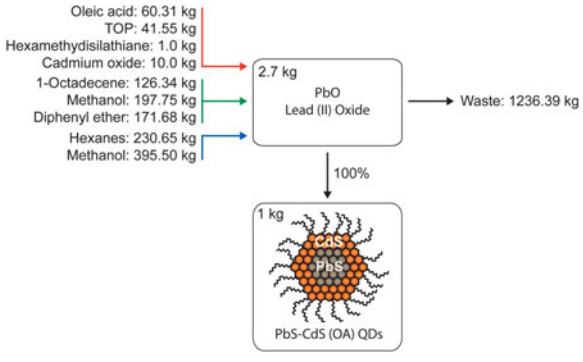


Figure 7. Synthesis of core–shell PbS-CdS quantum dots (QDs). The flowchart describes the synthesis of 1 kg of PbS-CdS core–shell QDs. The requisite quantities of (red arrow) reagent; (green arrow) solvents; and (blue arrow) workup ("crash out") materials are indicated for this single-step process. Note that a quantitative yield is assumed, as discussed in the caption of Table I.

https://doi.org/10.1557/mrs.2013.181 Published online by Cambridge University Press

Table I. Calculated large-scale chemical synthesis costs for red- and near-infrared-emitting quantum dots (QDs) and for two archetypal organic dyes.

Compound	References	Steps	Reagents ($ g^{-1})	Solvent ($ g^{-1})	Workup ($ g^{-1})	Total (w/o workup)		Total (w/workup)	
						($ g^{-1})	($ m^{-2})	($ g^{-1})	($ m^{-2})
"Legacy" CdSe (TOPO) QD	81	1	298.22	271.14	90.82	569.36	35.35	660.18	40.99
"Modern" CdSe (TOPO) QD*	16	1	42.41	15.3	1.62	57.71	3.35	59.34	3.44
"Legacy" CdSe-ZnS (TOPO) QD	82	1	1,613.13	271.14	111.48	1,884.27	105.37	1,995.76	111.60
"Modern" CdSe-CdS (TOPO) QD*	16	1	45.23	16.12	3.24	61.34	4.11	64.59	4.33
PbS (OA) QD, Method 1	101	1	14.66	3.25	11.08	17.90	1.29	28.98	2.09
PbS (OA) QD, Method 2*	18	1	36.00	8.99	22.51	44.99	3.24	67.50	4.86
PbS-CdS (OA) QD*	18	1	49.62	18.39	29.26	68.01	4.27	97.27	6.11
Alq_3	102	1	0.44	0.00	3.90	0.44	–	4.34	–
$Ir(ppy)_2(acac)$	103	1	621.66	35.86	639.26	657.52	–	1,296.78	–

Cost-per-gram for "legacy" CdSe QDs (with trioctylphosphine oxide (TOPO) ligands); "modern" CdSe QDs (TOPO ligands; wurtzite-CdSe synthesis); "legacy" CdSe-ZnS core–shell QDs (TOPO ligands); "modern" CdSe-CdS core–shell QDs (TOPO ligands; wurtzite-CdSe synthesis); PbS (via two methods) and PbS-CdS core–shell QDs (oleic acid ligands); fluorescent dye, tris(8-hydroxyquinolinato) aluminium (Alq_3); and phosphorescent dye, acetylacetonatobis(2-phenylpyridine) iridium ($Ir(ppy)_2(acac)$). The cost analysis accounts for all material inputs (reagents, solvents, and workup ["crash out"]), yielding total costs-per-gram both without and with workup. For the QDs, these have been converted into costs-per-area assuming a QD film of 25 nm thickness, as detailed in the text. *In the absence of literature yields, we assume quantitative yields; although this is clearly a slight over-estimate, it is a reasonable approximation given the synthetic refinements and waste recycling that will surely accompany scale-ups in QD synthesis.

significantly smaller quantities of more economical input materials, notably a significantly cheaper and air-stable source of Cd (cadmium oxide replaces dimethyl cadmium). These advances carry forward to the "modern" CdSe-CdS core–shell QDs ($61–65 g^{-1}), which cost only fractionally more than their core-only equivalents, again owing to the use of an economical source of Cd for the shell. In contrast, the "legacy" CdSe-ZnS core–shell QDs ($1884–1996 g^{-1}) inherit the 10-fold higher costs of their starting CdSe QDs and require the use of an expensive source of zinc for their shell (replacement of dimethyl zinc is key to lower costs). It is possible that reports of QD costs of up to $10,000 g^{-1} (Reference 9) may result from evaluation of antiquated "legacy" syntheses rather than more economical state-of-the-art approaches. The materials costs of NIR-emitting QDs (PbS, Method 1: $18–29 g^{-1}; PbS, Method 2: $45–68 g^{-1}; and PbS-CdS: $68–97 g^{-1}) are roughly commensurate with those of the "modern" visible-emitting QDs.

Current target prices for QDs synthesized via scaled-up continuous processes are ~$10 g^{-1} (Reference 21). As a guide, the materials cost of Alq_3—an archetypal organic dye used in OLEDs since the 1980s, and therefore subject to considerable economies of scale—is ~$4 g^{-1} (Reference 80). However, most heavy-metal-based phosphors found in high-performance OLEDs are considerably more expensive. A representative example is $Ir(ppy)_2(acac)$ (Reference 83), for which we calculate a materials cost of $658–1297 g^{-1}. Nevertheless, direct comparison of the materials costs of QDs with those of organic dyes is complicated by the specifics of a given application, which determine how much material is consumed. Considerations include whether it is used as a neat film or as a dopant dispersed in a host matrix, the thickness of such a film, and the wastefulness of the deposition technique employed. As is to be expected, the first QD-based products address optical down-conversion by using a compact edge-mounted geometry[10] (Figure 1b, inset) that requires relatively small amounts of QDs (often dispersed to maximize η_{PL}).

One way to try to assess our results is to translate them into approximate materials costs-per-unit-area (Table I). The per-area costs are based on the assumption that a typical QLED might comprise a 25 nm film of hexagonally close-packed QDs separated by ~0.5 nm due to their surrounding organic ligands. As expected, we obtain similar values for "modern" CdSe ($3 m^{-2}) and CdSe-CdS ($4 m^{-2}) QDs as for PbS (Method 1: $1–2 m^{-2}; Method 2: $3–5 m^{-2}) and PbS-CdS ($4–6 m^{-2}) QDs. "Legacy" CdSe and CdSe-ZnS QDs are significantly more expensive ($35–41 m^{-2} and $90–95 m^{-2}, respectively). Especially given the likelihood that QD syntheses will be subject to some economies-of-scale,[9] this is competitive, for example, with the DOE's 2015 SSL target cost of organic materials of $40 m^{-2} for OLEDs.[84] Moreover, this is just one possible metric, which does not necessarily reflect the higher material costs that luxury items such as displays might be able to shoulder.

One significant assumption that has so far been made, however, is that we can deposit QDs with 100% efficiency. In reality, the spin-casting technique (and therefore microcontact printing, which in published studies involves a spin-casting step) that has so far dominated laboratory demonstrations of QLEDs wastes ~95% of the starting solution.[85] Unless the QD

https://doi.org/10.1557/mrs.2013.181 Published online by Cambridge University Press

waste is recyclable, the associated 20-fold increase in QD materials costs could render some applications economically unviable. This points to the importance of developing low-waste QD-deposition techniques. For example, ink-jet printing of multi-colored pixel arrays of QDs for both down-conversion[86] and RGB QLED[85] technologies has been demonstrated, but further refinements in film quality and device performance are required.

Outlook

The unique optical traits of QDs lie at the heart of their appeal. Optoelectronic simulations, *in situ* measurements of devices, and tailored QD chemistry and LED design cannot only build on the significant efficiency gains achieved in QLEDs over the past two decades, but also further our understanding of their operating mechanisms and, most crucially, improve their operating lifetimes. The competitive economics of QD synthesis identified here reaffirms their outstanding potential as efficient sources of color-tunable light.

Acknowledgments

This article is based on work supported by the Center for Excitonics, an Energy Frontier Research Center funded by the US Department of Energy, Office of Science, Office of Basic Energy Sciences, under Award Number DE-SC0001088. K.W.S. acknowledges support from an NSF Graduate Research Fellowship.

References

1. Y. Shirasaki, G.J. Supran, M.G. Bawendi, V. Bulović, *Nat. Photonics* **7**, 13 (2013).
2. D.J. Norris, M.G. Bawendi, L.E. Brus, *Molecular Electronics: A "Chemistry for the 21st Century" Monograph, Chap. 9* (Blackwell Science, NY, 1997).
3. P.O. Anikeeva, J.E. Halpert, M.G. Bawendi, V. Bulović, *Nano Lett.* **9**, 2532 (2009).
4. Y.H. Niu, A.M. Munro, Y.-J. Cheng, Y.Q. Tian, M.S. Liu, J.L. Zhao, J.A. Bardecker, I. Jen-La Plante, D.S. Ginger, A.K.-Y. Jen, *Adv. Mater.* **19**, 3371 (2007).
5. L. Qian, Y. Zheng, J. Xue, P.H. Holloway, *Nat. Photonics* **5**, 543 (2011).
6. Q. Sun, Y.A. Wang, L.S. Li, D. Wang, T. Zhu, J. Xu, C. Yang, Y. Li, *Nat. Photonics* **1**, 717 (2007).
7. J. Kwak, W.K. Bae, D. Lee, I. Park, J. Lim, M. Park, H. Cho, H. Woo, D. Yoon, K. Char, S. Lee, C. Lee, *Nano Lett.* **12**, 2362 (2012).
8. V. Wood, V. Bulović, *Nano Reviews* **1**, 5202, doi: 10.3402/nano.v1i0.5202 (2010).
9. K. Bourzac, *Nature* **493**, 283 (2013).
10. S. Coe-Sullivan, W. Liu, P. Allen, J.S. Steckel, *ECS J. Solid State Sci. Technol.* **2**, R3026 (2013).
11. J.A. Chen, "High-Efficiency Wide-Color-Gamut Solid-State Backlight System for LCDs Using Quantum-Dot Enhancement Film," *SID Display Week 2012* (2012).
12. L. Sun, J.J. Choi, D. Stachnik, A.C. Bartnik, B.-R. Hyun, G.G. Malliaras, T. Hanrath, F.W. Wise, *Nat. Nanotechnol.* **7**, 369 (2012).
13. G. Konstantatos, C. Huang, L. Levina, Z. Lu, E.H. Sargent, *Adv. Funct. Mater.* **15**, 1865 (2005).
14. G.J. Supran, K.W. Song, G.W. Hwang, R.E. Correa, J. Scherer, E.A. Dauler, Y. Shirasaki, M.G. Bawendi, V. Bulović, "High-Efficiency and Brightness Near-Infrared Quantum-Dot LEDs Using Core-Shell (PbS-CdS) Colloidal Quantum-Dots," presented at the MRS Spring Meeting, San Francisco, CA (2013).
15. J.A. Hollingsworth, V.I. Klimov, *Nanocrystal Quantum Dots, Second Edition* (CRC Press, NY, 2010).
16. O. Chen, J. Zhao, V.P. Chauhan, J. Cui, C. Wong, D.K. Harris, H. Wei, H.-S. Han, D. Fukumura, R.K. Jain, M.G. Bawendi, *Nat. Mater.* **12**, 1 (2013).
17. J.R. Sommer, R.T. Farley, K.R. Graham, Y. Yang, J.R. Reynolds, J. Xue, K.S. Schanze, *ACS Applied Materials & Interfaces* **1**, 274 (2009).
18. J.M. Pietryga, D.J. Werder, D.J. Williams, J.L. Casson, R.D. Schaller, V.I. Klimov, J.A. Hollingsworth, *J. Am. Chem. Soc.* **130**, 4879 (2008).
19. E.H. Sargent, *Adv. Mater.* **17**, 515 (2005).
20. A.L. Rogach, A. Eychmüller, S.G. Hickey, S.V. Kershaw, *Small* **3**, 536 (2007).
21. J. Oliver, BCC Research paper NAN027C, *Quantum Dots: Global Market Growth and Future Commercial Prospects* (2011).
22. www.displaysearch.com.
23. V.L. Colvin, M.C. Schlamp, A.P. Alivisatos, *Nature* **370**, 354 (1994).
24. B.O. Dabbousi, M.G. Bawendi, O. Onitsuka, M.F. Rubner, *Appl. Phys. Lett.* **66**, 1316 (1995).
25. S. Coe, W.-K. Woo, M.G. Bawendi, V. Bulović, *Nature* **420**, 800 (2002).
26. L. Kim, P.O. Anikeeva, S.A. Coe-Sullivan, J.S. Steckel, M.G. Bawendi, V. Bulović, *Nano Lett.* **8**, 4513 (2008).
27. J.S. Steckel, P. Snee, S. Coe-Sullivan, J.P. Zimmer, J.E. Halpert, P. Anikeeva, L.-A. Kim, V. Bulović, M.G. Bawendi, *Angew. Chem.* **45**, 5796 (2006).
28. A. Rizzo, M. Mazzeo, M. Palumbo, G. Lerario, S. D'Amone, R. Cingolani, G. Gigli, *Adv. Mater.* **20**, 1886 (2008).
29. A.H. Mueller, M.A. Petruska, M. Achermann, D.J. Werder, E.A. Akhadov, D.D. Koleske, M.A. Hoffbauer, V.I. Klimov, *Nano Lett.* **5**, 1039 (2005).
30. M. Achermann, M.A. Petruska, S. Kos, D.L. Smith, D.D. Koleske, V.I. Klimov, *Nature* **429**, 642 (2004).
31. M.J. Panzer, K.E. Aidala, P.O. Anikeeva, J.E. Halpert, M.G. Bawendi, V. Bulović, *Nano Lett.* **10**, 2421 (2010).
32. P.O. Anikeeva, C.F. Madigan, J.E. Halpert, M.G. Bawendi, V. Bulović, *Phys. Rev. B* **78**, 085434 (2008).
33. R.H. Friend, R.W. Gymer, A.B. Holmes, J.H. Burroughes, R.N. Marks, C. Taliani, D.D.C. Bradley, D.A. Dos Santos, J.L. Bredas, M. Lögdlund, W.R. Salaneck, *Nature* **397**, 121 (1999).
34. P.E. Burrows, V. Bulović, S.R. Forrest, L.S. Sapochak, D.M. McCarty, *Appl. Phys. Lett.* **65**, 2922 (1994).
35. J.M. Caruge, J.E. Halpert, V. Wood, V. Bulović, M.G. Bawendi, *Nat. Photonics* **2**, 247 (2008).
36. V. Wood, M.J. Panzer, J.E. Halpert, J.-M. Caruge, M.G. Bawendi, V. Bulović, *ACS Nano* **3**, 3581 (2009).
37. S.H. Cho, J. Sung, I. Hwang, R.H. Kim, Y.S. Choi, S.S. Jo, T.W. Lee, C. Park, *Adv. Mater.* **24**, 4540 (2012).
38. J.W. Stouwdam, R.A.J. Janssen, *J. Mater. Chem.* **18**, 1889 (2008).
39. J.-M. Caruge, J.E. Halpert, V. Bulović, M.G. Bawendi, *Nano Lett.* **6**, 2991 (2006).
40. B.S. Mashford, M. Stevenson, Z. Popovic, C. Hamilton, Z. Zhou, C. Breen, J. Steckel, V. Bulović, M.G. Bawendi, S. Coe-Sullivan, P.T. Kazlas, *Nat. Photonics* **7**, 407 (2013).
41. R. Meerheim, S. Scholz, S. Olthof, G. Schwartz, S. Reineke, K. Walzer, K. Leo, *J. Appl. Phys.* **104**, 014510 (2008).
42. R. Meerheim, M. Furno, S. Hofmann, B. Lüssem, K. Leo, *Appl. Phys. Lett.* **97**, 253305 (2010).
43. T.-H. Kim, K.-S. Cho, E.K. Lee, J.S. Lee, J. Chae, J.W. Kim, D.H. Kim, J.-Y. Kwon, G. Amaratunga, S.Y. Lee, B.L. Choi, Y. Kuk, J.M. Kim, K. Kim, *Nat. Photonics* **5**, 176 (2011).
44. P.O. Anikeeva, J.E. Halpert, M.G. Bawendi, V. Bulović, *Nano Lett.* **7**, 2196 (2007).
45. Y.Q. Li, A. Rizzo, R. Cingolani, G. Gigli, *Adv. Mater.* **18**, 2545 (2006).
46. S. Coe-Sullivan, OECD/NNI Symposium, QD Vision, Inc. presenting work from AFOSR grant number FA9550–07-C-0056 (2012).
47. G. Qian, Z. Zhong, M. Luo, D. Yu, Z. Zhang, Z.Y. Wang, D. Ma, *Adv. Mater.* **21**, 111 (2009).
48. E.J.D. Klem, L. Levina, E.H. Sargent, *Appl. Phys. Lett.* **87**, 053101 (2005).
49. Y.T. Lim, S. Kim, A. Nakayama, N.E. Stott, M.G. Bawendi, J.V. Frangioni, *Mol. Imaging* **2**, 50 (2003).
50. S. Kim, Y.T. Lim, E.G. Soltesz, A.M. De Grand, J. Lee, A. Nakayama, J.A. Parker, T. Mihaljevic, R.G. Laurence, D.M. Dor, L.H. Cohn, M.G. Bawendi, J.V. Frangioni, *Nat. Biotechnol.* **22**, 93 (2004).
51. I.L. Medintz, H.T. Uyeda, E.R. Goldman, H. Mattoussi, *Nat. Mater.* **4**, 435 (2005).
52. M.F. Frasco, N. Chaniotakis, *Sensors* **9**, 7266 (2009).
53. N. Tessler, V. Medvedev, M. Kazes, S. Kan, U. Banin, *Science* **295**, 1506 (2002).
54. K.N. Bourdakos, D.M.N.M. Dissanayake, T. Lutz, S.R.P. Silva, R.J. Curry, *Appl. Phys. Lett.* **92**, 153311 (2008).
55. L. Bakueva, S. Musikhin, M.A. Hines, T.-W.F. Chang, M. Tzolov, G.D. Scholes, E.H. Sargent, *Appl. Phys. Lett.* **82**, 2895 (2003).
56. K.R. Choudhury, D.W. Song, F. So, *Org. Electron.* **11**, 23 (2010).
57. O. Solomeshch, A. Kigel, A. Saschiuk, V. Medvedev, A. Aharoni, A. Razin, Y. Eichen, U. Banin, E. Lifshitz, N. Tessler, *J. Appl. Phys.* **98**, 074310 (2005).
58. G.J. Supran, K.W. Song, G.W. Hwang, R.E. Correa, J. Scherer, E.A. Dauler, Y. Shirasaki, M.G. Bawendi, V. Bulović, Patent Application 61/735, 344 (2012).
59. K.-Y. Cheng, R. Anthony, U.R. Kortshagen, R.J. Holmes, *Nano Lett.* **10**, 1154 (2010).
60. K.-Y. Cheng, R. Anthony, U.R. Kortshagen, R.J. Holmes, *Nano Lett.* **11**, 1952 (2011).
61. Y.Q. Zhang, X.A. Cao, *Appl. Phys. Lett.* **97**, 253115 (2010).
62. W.K. Bae, J. Kwak, J. Lim, D. Lee, M.K. Nam, K. Char, C. Lee, S. Lee, *Nano Lett.* **10**, 2368 (2010).
63. P. Jing, J. Zheng, Q. Zeng, Y. Zhang, X. Liu, X. Liu, X. Kong, J. Zhao, *J. Appl. Phys.* **105**, 044313 (2009).

https://doi.org/10.1557/mrs.2013.181 Published online by Cambridge University Press

64. Y. Shirasaki, G.J. Supran, W.A. Tisdale, V. Bulović, *Phys. Rev. Lett.* **110**, 217403 (2013).
65. D. Bozyigit, O. Yarema, V. Wood, *Adv. Funct. Mater.* **23**, 3024 (2013).
66. J. Zhao, J.A. Bardecker, A.M. Munro, M.S. Liu, Y. Niu, I.-K. Ding, J. Luo, B. Chen, A.K.-Y. Jen, D.S. Ginger, *Nano Lett.* **6**, 463 (2006).
67. J.W. Stouwdam, R.A.J. Janssen, *Adv. Mater.* **21**, 2916 (2009).
68. H. Huang, A. Dorn, G.P. Nair, V. Bulović, M.G. Bawendi, *Nano Lett.* **7**, 3781 (2007).
69. Z.-B. Wang, H.-C. Zhang, J.-Y. Zhang, *Chin. Phys. Lett.* **27**, 127803 (2010).
70. L. Sun, A. Bartnik, B. Hyun, F. Wise, J. Reed, J. Slinker, G. Malliaras, Y. Zhong, L. Bao, H. Abruna, *Conference on Lasers and Electro-Optics* (Optical Society of America), paper CThS6, doi:10.1109/CLEO.2008.4551522 (2008).
71. W.-K. Woo, K.T. Shimizu, M.V. Jarosz, R.G. Neuhauser, C.A. Leatherdale, M.A. Rubner, M.G. Bawendi, *Adv. Mater.* **14**, 1068 (2002).
72. C. Galland, Y. Ghosh, A. Steinbrück, M. Sykora, J.A. Hollingsworth, V.I. Klimov, H. Htoon, *Nature* **479**, 203 (2011).
73. A. Pandey, P. Guyot-Sionnest, *J. Phys. Chem. Lett.* **1**, 45 (2010).
74. T.-W.F. Chang, S. Musikhin, L. Bakueva, L. Levina, M.A. Hines, P.W. Cyr, E.H. Sargent, *Appl. Phys. Lett.* **84**, 4295 (2004).
75. M. Achermann, M.A. Petruska, D.D. Koleske, M.H. Crawford, V.I. Klimov, *Nano Lett.* **6**, 1396 (2006).
76. A. Shik, G. Konstantatos, E.H. Sargent, H.E. Ruda, *J. Appl. Phys.* **94**, 4066 (2003).
77. S. Coe-Sullivan, "M-5: Nanotechnology for Displays: A Potential Breakthrough for OLED Displays and LCDs (QD Vision, Inc.)," Display Week 2012.
78. K.-S. Cho, E.K. Lee, W. Joo, E. Jang, T. Kim, S.J. Lee, S. Kwon, J.Y. Han, B. Kim, B.L. Choi, J.M. Kim, *Nat. Photonics* **3**, 341 (2009).
79. R. Meerheim, S. Scholz, S. Olthof, G. Schwartz, S. Reineke, K. Walzer, K. Leo, *J. Appl. Phys.* **104**, 014510 (2008).
80. T.P. Osedach, T.L. Andrew, V. Bulović, *Energy Environ. Sci.* **6**, 711 (2013).
81. C.B. Murray, D.J. Norris, M.G. Bawendi, *J. Am. Chem. Soc.* **115**, 8706 (1993).
82. M.A. Hines, P. Guyot-Sionnest, *J. Phys. Chem.* **100**, 468 (1996).
83. M.G. Helander, Z.B. Wang, J. Qiu, M.T. Greiner, D.P. Puzzo, Z.W. Liu, Z.H. Lu, *Science* **332**, 944 (2011).
84. US Department of Energy, "Solid-State Lighting Research and Development: Manufacturing Roadmap" (2012).
85. H.M. Haverinen, R.A. Myllylä, G.E. Jabbour, *J. Display Technol.* **6**, 87 (2010).
86. M.J. Panzer, V. Wood, S.M. Geyer, M.G. Bawendi, V. Bulović, *J. Display Technol.* **6**, 90 (2010).
87. J.J. Shiang, A.V. Kadavanich, R.K. Grubbs, A.P. Alivisatos, *J. Phys. Chem.* **99**, 17417 (1995).
88. B.O. Dabbousi, M.G. Bawendi, O. Onitsuka, M.F. Rubner, *Appl. Phys. Lett.* **66**, 1316 (1995).
89. H. Mattoussi, L.H. Radzilowski, B.O. Dabbousi, E.L. Thomas, M.G. Bawendi, M.F. Rubner, *J. Appl. Phys.* **83**, 7965 (1998).
90. M.C. Schlamp, X. Peng, A.P. Alivisatos, *J. Appl. Phys.* **82**, 5837 (1997).
91. S. Coe-Sullivan, J.S. Steckel, W.-K. Woo, M.G. Bawendi, V. Bulović, *Adv. Funct. Mater.* **15**, 1117 (2005).
92. S. Coe-Sullivan, "12.2: Quantum-Dot Light-Emitting Diodes for Near-to-Eye and Direct-View Display Applications (QD Vision, Inc.)," Display Week 2011.
93. C.W. Tang, S.A. VanSlyke, C.H. Chen, *J. Appl. Phys.* **65**, 3610 (1989).
94. Y. Hamada, H. Kanno, T. Tsujioka, H. Takahashi, T. Usuki, *Appl. Phys. Lett.* **75**, 1682 (1999).
95. B. Chen, X. Lin, L. Cheng, C.-S. Lee, W.A. Gambling, S.T. Lee, *J. Phys. D: Appl. Phys.* **34**, 30 (2001).
96. M. Leung, C.-C. Chang, M.-H. Wu, K.-H. Chuang, J.-H. Lee, S.-J. Shieh, S.-C. Lin, C.-F. Chiu, *Org. Lett.* **8**, 2623 (2006).
97. J.S. Steckel, S. Coe-Sullivan, V. Bulovic, M.G. Bawendi, *Adv. Mater.* **15**, 1862 (2003).
98. D.S. Koktysh, N. Gaponik, M. Reufer, J. Crewett, U. Scherf, A. Eychmüller, J.M. Lupton, A.L. Rogach, J. Feldmann, *ChemPhysChem* **5**, 1435 (2004).
99. É. O'Connor, A. O'Riordan, H. Doyle, S. Moynihan, A. Cuddihy, G. Redmond, *Appl. Phys. Lett.* **86**, 201114 (2005).
100. X. Ma, F. Xu, J. Benavides, S.G. Cloutier, *Org. Electron.* **13**, 525 (2012).
101. N. Zhao, T.P. Osedach, L.-Y. Chang, S.M. Geyer, D. Wanger, M.T. Binda, A.C. Arango, M.G. Bawendi, V. Bulović, *ACS Nano* **4**, 3743 (2010).
102. T. Horihata, K. Okamoto, J. Hidaka, H. Einaga, *Bull. Chem. Soc. Jpn.* **61**, 2999 (1988).
103. M. Furugori, S. Igawa, J. Kamatani, S. Miura, H. Mizutani, T. Moriyama, S. Okada, T. Takiguchi, A. Tsuboyama, *Metal Coordination Compound and Electroluminescence Device*, US Patent 20030235712 (2003).
104. US Department of Health and Human Services, "Toxicological Profile for Cadmium" (2012).
105. K.-H. Lee, J.-H. Lee, W.-S. Song, H. Ko, C. Lee, J.-H. Lee, H. Yang, *ACS Nano*, doi: 10.1021/nn402870e (2012). □



https://doi.org/10.1557/mrs.2013.181 Published online by Cambridge University Press